Progress In Electromagnetics Research B, Vol. 51, 389–406, 2013

IMPROVING CONVERGENCE TIME OF THE ELECTROMAGNETIC INVERSE METHOD BASED ON GENETIC ALGORITHM USING THE PZMI AND NEURAL NETWORK

Sofiene Saidi* **and Jaleleddine Ben Hadj Slama**

SAGE, National Engineering School of Sousse, (ENISo), University of Sousse, Technopole of Sousse, Sousse 4054, Tunisia

Abstract—In this paper we present a methodology to guarantee the convergence of the electromagnetic inverse method. This method is applied to electromagnetic compatibility (EMC) in order to overcome the difficulties of measuring the radiated electromagnetic field and to reduce the cost of the EMC analysis. It consists in using Genetic Algorithms (GA) to identify a model that will be used to estimate the electric and magnetic field radiated by the device under test. This method is based on the recognition of the equivalent radiation sources using the Near Field (NF) cartography radiated by the device. Our contribution in this field is to improve the ability and the convergence of the electromagnetic inverse method by using the Pseudo Zernike Moment Invariant (PZMI) descriptor and the Artificial Neural Network (ANN). The validation of the proposed method is performed using the NF emitted by known electric and magnetic dipoles. Our results have proved that the proposed method guarantees the convergence of the electromagnetic inverse method and that the convergence speeds up while retaining all the other performances.

1. INTRODUCTION

The rapid development of electrical systems has created the need to analyze and control their electromagnetic radiation. Therefore, the knowledge of the electromagnetic field distribution of any electrical device is necessary. Since the electrical device is composed by complex and active components, the computation of the Near Field (NF) and Far Field (FF) has many difficulties. A new technique, called the Near Field (NF) technique, has been developed to overcome this problem.

Received 16 September 2012, Accepted 29 April 2013, Scheduled 15 May 2013

* Corresponding author: Sofiene Saidi (saidi.sofiene@yahoo.fr).

The measurement of the electromagnetic NF is made with a good signal-to-noise ratio (S/N) because it is taken in a region very close to the radiation source. Thus, it does not require a particular measurement environment such as those required when measuring the electromagnetic FF (anechoic chamber). In addition, the NF cartography is directly related to the device geometry (the positions of radiation sources).

The electromagnetic inverse method is based on the NF technique [1, 2]. A model of a microcontroller has been described by electric dipoles using measurements of the magnetic NF components H_x and H_y. This model was created by inverting the matrix and it can calculate only the magnetic field [3]. This model was improved by coupling the digital image processing technique with the optimization algorithm [4]. In order to predict the magnetic and electric NF, [5, 6] developed a model based on a network of electric and magnetic dipoles.

The resolution with the inverse electromagnetic method requires an optimization method such as the Genetic Algorithms (GA) [7]. In [8] an adaptive GA was applied to model a DC-DC converter. [9] used a binary GA optimization method to simulate wire and resonator antennas. Another study [10] considered that loops were the mainly radiation sources in circuits and used the GA to identify the rectangular loops in the circuit.

The study [11] shows that the optimization method based on GA is the most powerful in terms of accuracy compared to that based on the Fast Fourier Transform (FFT) or on an integral equation.

The convergence of the electromagnetic inverse method based on the GA requires a significant calculation time. The GA method is characterized by several parameters. A judicious choice of these parameters can accelerate the convergence of this method. In a previous work [12], we explored some parameters that can influence the efficiency of the convergence of the electromagnetic inverse method based on the GA. These parameters are: the population size, the crossover rate, the selection function, and the fitness function. So, a judicious choice of these parameters can accelerate the convergence of the electromagnetic inverse method to the final solution in a shorter time. In order to adapt this method to the electronic power system, [7] coupled the electromagnetic inverse method with a numerical method: the Moments Method (MoM). This new approach demonstrates the ability of this coupling in modeling the radiation of large circuits such as those used in power electronic systems.

In this work, we propose to improve the electromagnetic inverse method based on the GA. Our contribution consists in coupling the latter method with a powerful technique. This technique, called the

Pseudo Zernike Moment Invariant (PZMI), has been used in the recent years in the digital image processing and faces recognition,thanks to its superior future representation capability [13]. The PZMI vector is applied, in our case, to represent the radiated NF as a complex vector. The proposed methodology has coupled different methods used in the literature: image processing, the GA and the Neural Network (NN). It has at least three main advantages when comparing it to other approaches [3]: firstly, it guarantees the convergence of the electromagnetic inverse method and it speeds up the convergence; secondly, it makes the source identification using the magnitude of only one component of the magnetic field (H_z); and finally, it works even if all the dipoles parameters are not known.

In this paper, we will describe the electromagnetic inverse method based on the GA in Section 2. In Section 3, we will introduce the proposed approach. Consequently, we will explain the choice of the used scan-window as well as the application of the PZMI descriptor with the Neural Network to classify the radiation sources. In Section 4, we will describe the implementation of the proposed method and the obtained results when using an NF cartography radiated by an important number of dipoles. In order to examine the ability of our contribution we will compare results to those obtained using the classical method. Finally, we will focus on the robustness of the proposed method.

2. THE ELECTROMAGNETIC INVERSE METHOD BASED ON GENETIC ALGORITHMS

The electromagnetic inverse method consists in using NF measurements to modelize the studied system by a network of electric or magnetic dipoles or both of them. The modeling procedure is resumed in three steps (Figure 1). First, the NF measurements are made at an h height which is very low compared to $\frac{\lambda}{2\pi}$ ($\frac{\lambda}{2\pi}$ is the limit between the NF and the FF, where λ is the wavelength). Therefore, the NF presented as a cartography, which allows us to locate the regions of the high or low electromagnetic field radiated by an electronic board. In this study, we have chosen the vertical component of the magnetic field H_z. However we can apply the method with the other magnetic field components H_x and H_y. In a second step, using the measured NF, the GA proceeds to seek for optimum parameters of the dipoles (magnetic moments, positions and orientations) that will give a calculated field which is closer to the measured NF. In a third step, the identified parameters are used to estimate the electromagnetic field emitted at any point in the space. The optimization fitness function (1) that we have

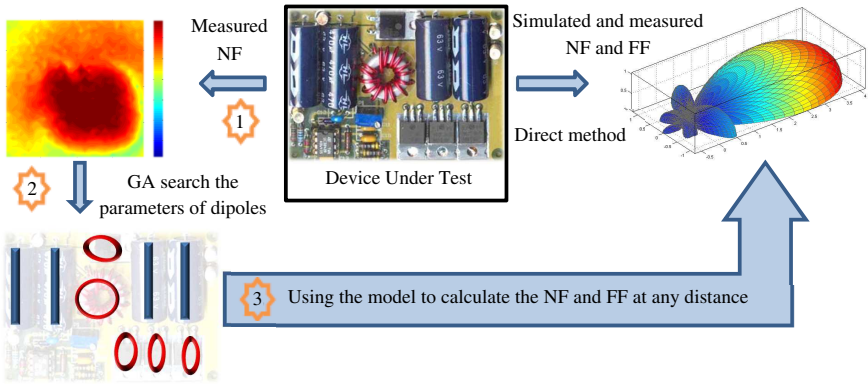

Figure 1. The electromagnetic inverse method based on the GA.

used to provide a comparison between the measured and the estimated NF is the Euclidean distance between the two cartographies.

$$F = \sum |NF_{\text{measured}} - NF_{\text{calculated}}| \tag{1}$$

Also, to overcome problems related to measurement errors when doing validations, we have applied in this work the proposed methodology only to the cartographies of the calculated NF values.

An elementary magnetic or electric radiating dipole (Figure 2) is characterized by a set of parameters. That is why a dipole can be represented by a d_i vector which includes all the parameters $d_i = (T_d, M_d, X_d, Y_d, Z_d, \theta, \varphi)$, where T_d is the type of dipole, M_d is the magnetic moment, (X_d, Y_d, Z_d) is the dipole position and θ, φ is the dipole orientation.

The magnetic field H_z radiated by the two elementary dipoles is described with the analytical Equations (2) and (3).

For the electric dipole:

$$H_Z = \frac{j\cdot k\cdot M_d}{4\cdot\pi\cdot R}\cdot\psi(R)\cdot\left(1+\frac{1}{j\cdot k\cdot R}\right)\cdot\begin{pmatrix}\sin(\theta)\sin(\varphi)\cdot(Yde-Y0)\\-\sin(\theta)\cos(\varphi)\cdot(Xde-X0)\end{pmatrix} \tag{2}$$

and for the magnetic dipole:

$$H_Z = -\frac{k^2}{4}\psi(R)\cdot M_d\cdot\begin{bmatrix}\left(\left(1+\frac{1}{j\cdot k\cdot R}+\frac{1}{(j\cdot k\cdot R)^2}\right)\cdot\cos(\theta)\right)\\-\left(\left(1+\frac{3}{j\cdot k\cdot R}+\frac{3}{(j\cdot k\cdot R)^2}\right)\cdot\frac{1}{R^2}\cdot(Zde-Z0)\right)\\\cdot\begin{pmatrix}\cos(\theta)(Zde-Z0)\\+\sin(\theta)\cos(\varphi)(Yde-Y0)\\+\sin(\theta)\sin(\varphi)\cdot(Xde-X0)\end{pmatrix}\end{bmatrix} \tag{3}$$

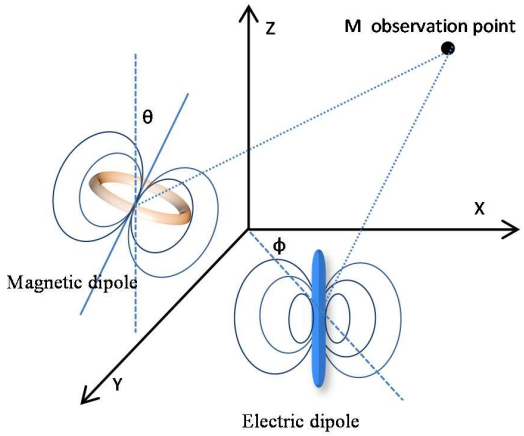

Figure 2. Electric and magnetic dipoles.

where $\psi(R)$ is the Green function, $k = \omega \cdot \sqrt{\varepsilon \cdot \mu}$ and $R = \sqrt{(Xde - X0)^2 + (Yde - Y0)^2 + (Zde - Z0)^2}$: the distance between the observation point and the dipole.

The vector $d_i = (T_d, M_d, X_d, Y_d, Z_d, \theta, \varphi)$ forms the population of Genetic Algorithms. The GA is a global optimization algorithm used for solving non-linear systems, and surely the linear ones. It is based on the evolutionary natural selection of Darwin. And it is composed of five steps: the initial population which is usually created randomly,the evaluation of this population using the fitness function, the selection of the current population for reproduction, the mutation,and the crossover to give the new improved population.

As mentioned in Section 1 of this paper, a judicious choice of GA parameters can accelerate the convergence of the inverse electromagnetic method. So in this work, we refer to [12] for choosing the optimal GA parameters in order to reduce the convergence time.

3. THE IMPROVED ELECTROMAGNETIC INVERSE METHOD

Due to the convergence problems of the classical electromagnetic inverse method, we have to exploit information issued from the NF cartography. The new method consists in modeling the human expertise in knowledge engineering. The general methodology of the proposed approach is presented as follows.

After introducing the NF measurements, the scan-window

algorithm extracts a local NF cartography using an appropriate window. Then the scan-window algorithm moves up the window until identifying two dipole parameters: the type (electric or magnetic) and the position (X_d, Y_d) [14]. The other parameters (magnetic moment M_d and the orientation θ and φ) will be identified by the GA.

The obtained dipole parameters are then used to calculate values of the radiated NF from the dipole. The calculated values are subtracted from the initial cartography. The above procedure is repeated until extracting and identifying of all the radiating sources (Figure 3).

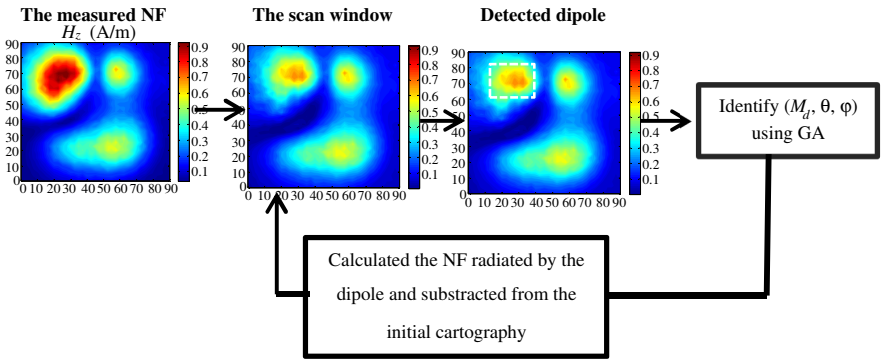

Figure 3. The improved electromagnetic inverse method.

The proposed method consists in using the GA as a subprogram to find three parameters (M_d, θ and φ) of one dipole whose position and type are identified with the scan-window algorithm. The latter is based on two algorithms: the PZMI descriptors and the NN.

3.1. The Scan-window Algorithm

The studied cartography is represented by a matrix containing measured amplitudes of the vertical component of the magnetic field. The cartography dimension usually depends on measuring parameters such as the size of the scan area, the distance between the probe and the studied system and the step between two acquisition points along horizontal directions. This cartography contains information about the distribution and amplitude of the electromagnetic NF radiated by the Device Under Test (DUT).

In order to achieve the purpose of our study, which consists in using the NF cartography to detect and identify the radiating sources, we propose to use the diagram given in Figure 4.

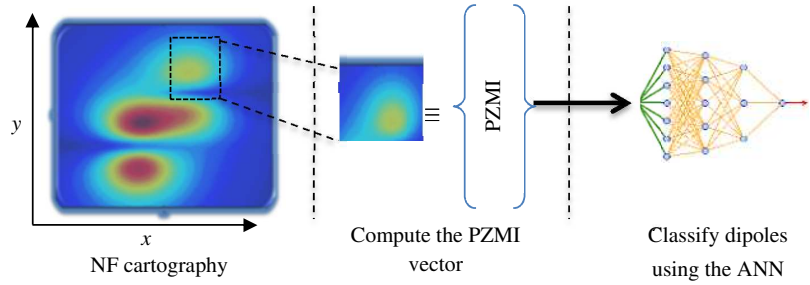

Figure 4. The *scan-window* algorithm.

In order to properly proceed with the NF cartography, we choose recent techniques used in the pattern of fingerprint recognition and identification: the PZMI descriptors and the Neural Network (NN). These techniques are based on extracting the vector characteristics of an image. This step consists in assimilating all the essential and relevant information of an image as a low dimensional moment vector. The main aim of this project is to reduce the amount of parameters to be determined by the GA. For this reason, we have decided to use the PZMI method.

3.2. The Scan-window Choice

The objective of this section is to justify the choice of the scan-window. Firstly, we define a suitable window on which we scan the

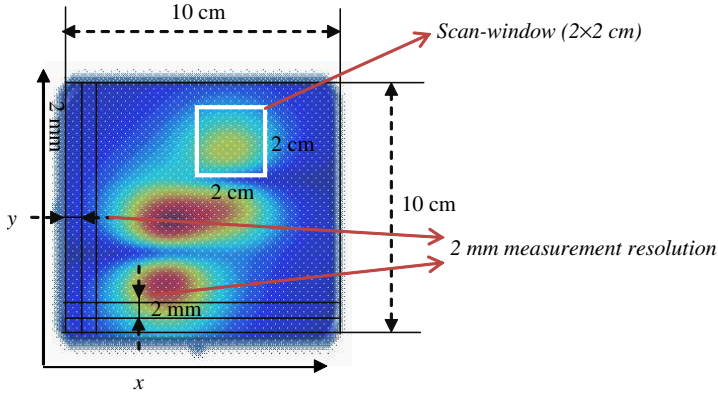

Figure 5. The *scan-window*.

NF cartography and then we use the scanned cartography to search a local dipole. The study [14] shows that the choice of the scan window depends on the measured cartography size, resolution and height. We suppose that in our scan window, we have only one dipole at maximum. To overcome the limitations of this hypothesis, we can extend the learning base with additional cases such as two or more dipoles at the same scan-window.

[13] approved, by using several cartographies for various configurations, that the ability of the method based on the PZMI would increase with the number of measurement points. Referring to [14], we have selected the optimal size of the scan-window. Consequently, we have chosen the measured cartography equal to $10 \times 10\,\text{cm}$ at an $h = 2\,\text{cm}$ height and with a measurement resolution equal to $2\,\text{mm}$ (Figure 5).

3.3. Pseudo-Zernike Moment Invariant

The Zernike moments are orthogonal complex moments that can describe an image by a complex vector. The amplitude of this vector is characterized byan invariance when rotating [15, 16].

In this method, the area is set by orthogonal pseudo-Zernike polynomials, defined as polar coordinates inside the unit circle. The two-dimensional pseudo-Zernike moment Z_{nm}, for an order n and a repetition m, is defined using an image intensity function $f(\rho, \theta)$ as given in Equations (4), (5) and (6).

$$Z_{nm} = \frac{n+1}{\pi} \sum_{x} \sum_{y} f(x,y)\, V^{*}_{nm}(x,y), \quad x^2 + y^2 \leq 1 \tag{4}$$

$$V_{nm} = R_{nm(\rho)} e^{-jm\theta} \tag{5}$$

where $\rho = \sqrt{x^2 + y^2}$, $\theta = \tan^{-1}(\frac{x}{y})$.

$$R_{nm(\rho)} = \sum_{s=0}^{\frac{n-|m|}{2}} (-1)^s \frac{(n-s)!}{s!\left(\frac{n+|m|}{2} - s\right)!\left(\frac{n-|m|}{2} - s\right)!} \rho^{n-2s} \tag{6}$$

Table 1. PZMI vector of order 4.

R_{nm}	$n=0$	$n=1$	$n=2$	$n=3$
$m=0$	1	$-2+3\rho$	$3+10\rho^2-12\rho$	$-4+35\rho^3-60\rho^2+30\rho$
$m=1$	0	ρ	$5\rho^2-4\rho$	$21\rho^3-302+10\rho$
$m=2$	0	0	ρ^2	$7\rho^3-6\rho^2$
$m=3$	0	0	0	ρ^3

where Z_{nm} is the moment of Zernike, V_{nm} the function of Zernike, and R_{nm} the radial polynomial of Zernike.

Using the previous equations, we calculate the PZMI vector of order 4 as described in (Table 1).

The PZMI vector of order 4 for the NF cartography has 9 complex numbers that describe amplitudes and phases. To evaluate the rotation invariance of the descriptor PZMI, we calculate the PZMI vector of the magnetic field radiated by a magnetic dipole for several orientations. First, in Figure 6, we give the cartographies of the z-component of the magnetic field radiated by a magnetic dipole for several orientations.

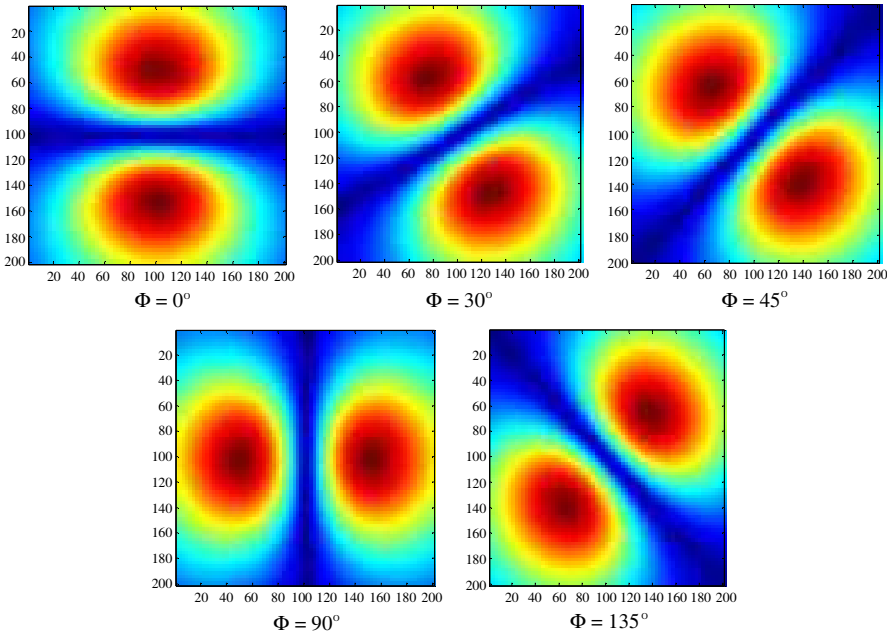

Figure 6. The cartographies of the z-component of the magnetic field radiated by a magnetic dipole for several orientations.

Afterwards, we determine the PZMI vector for all the NF cartographies. Table 2 represents only the amplitude of the PZMI vectors and the invariance rate $\sigma(\%)$.

The image of a cartography radiated by a dipole is easier to identify then that of a face. So, the identification of dipoles using cartography is not as complicated as the face recognition. The study of the PZMI vector invariance shows that with a moment order equal to 4, the PZMI can describe a dipole for different orientations with an accuracy equal to 90%. We notice that the left-over modulus is invariant whatever the orientation of the dipole is. This characteristic

Table 2. The PZMI vector of many orientations.

Φ		0°	30°	45°	90°	135°	σ(%)
PZMI Modulus	$\lvert -2+3\rho\rvert$	901.45	878.54	878.54	901.45	879.17	98.95
	$\lvert 3+10\rho^2-12\rho\rvert$	55.951	54.37	54.37	55.951	60.651	96.64
	$\lvert -4+35\rho^3 -60\rho^2+30\rho\rvert$	868.31	886.68	916.32	868.31	913.86	97.45
	$\lvert\rho\rvert$	235.99	331.55	363.16	235.99	359.04	77.33
	$\lvert 5\rho^2-4\rho\rvert$	33.329	34.142	33.078	33.329	35.189	78.53
	$\lvert 21\rho^3-302+10\rho\rvert$	34.7	34.834	37.97	34.7	39.826	91.48
	$\lvert\rho^2\rvert$	303.55	294.61	279.15	303.55	290.63	96.95
	$\lvert 7\rho^3-6\rho^2\rvert$	563.6	562.61	546.42	563.6	550.65	98.03
	$\lvert\rho^3\rvert$	264.12	189.41	149.9	264.12	145.16	76.72
Invariance rate							90.22%

can be useful to identify a dipole regardless of its orientation.

3.4. The Neural Network

In order to classify the radiating elements using the PZMI vector, we have chosen an algorithm usually used in pattern recognition and classification: the neural network. To achieve the purpose of our application using the NN, we have performed three stages:

- Choosing a suitable ANN structure.
- Preparing a training database.
- Validating the selected ANN.

- The ANN structure:

The choice of the structure of a Neural Network depends strongly on the type of the treated problem. Among the types of neural network, we have used the simplest structure which is the Multi-Layer Perceptron network (MLP): it contains an input, a hidden layer and an output one (Figure 7). The first one is the PZMI vector. It contains 9 neurons. [17] demonstrated that MLP with one provided hidden layer and an enough number of neurons could approximate any function with a good accuracy. The choice of the number of neurons in the hidden layer has an important effect on the efficiency of the NN. According to [18], the number of neurons in the hidden layer must be equal to that of the input one (9 neurons).

- The learning phase:

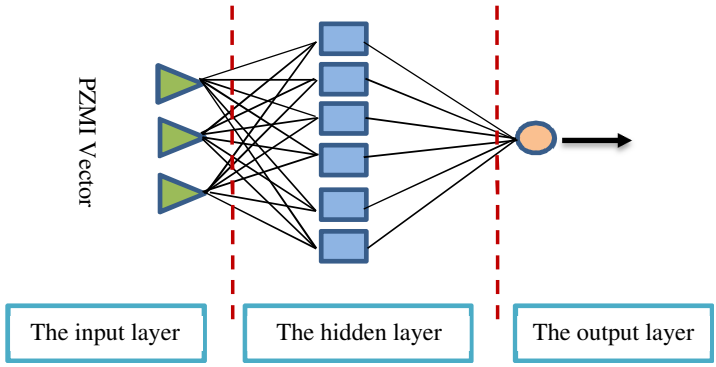

Figure 7. The MLP structure.

This stage consists in calculating the optimal w_i weights of the connections between the layers using a database which contains their inputs and outputs. The learning method is the back-propagation. To implement a neural network in our study, we have prepared a learning database including 1,158 PZMI vectors calculated from 1,158 different cartographies. To create this training base, we have proceeded by calculating the NF radiated by an electric and then magnetic dipole for different orientations. After that, we have calculated the PZMI for all the NF cartographies. All these calculation are made automatically using an appropriate routine that we have developed. 70% of this database have been used for creating the neural network and the remaining 30% has served for testing its ability. To characterize the electric and magnetic dipole having the same size, the distribution of the PZMI vectors is presented in Table 4. We have chosen the value "1" as an output for an electric dipole, "0" for a magnetic dipole and "0.5" for other cases of cartographies as shown in Table 3.

Table 3. The learning database.

The training base		output
Electric dipole	**370** (dipole orientation)	1
Magnetic dipole	**370** (dipole orientation)	0
No field or no magnetic or electric dipole	**70**	0.5
The test base		
348 PZMI vectors		

- The ANN validation:

To generalize the network for our application, we must validate the selected ANN with other cases of cartographies. This stage will be detailed in the next section.

4. IMPLEMENTATION OF THE INVERSE ELECTROMAGNETIC METHOD

In order to validate the ability of our proposed approaches, we will compare results obtained with the proposed methodology to those obtained with the classical electromagnetic inverse method based on GA. The stopping criteria of the GA is set at $fitness = 1\%$.

The first structure used for validation is constituted by 6 dipoles: 3 magnetic dipoles and 3 electric ones. The parameters of all the dipoles are given in Table 4.

Table 4. The parameters of 6 dipoles.

No	T_d	M_d	X_d, Y_d, Z_d (cm)	$\theta\,(^\circ)$	$\varphi\,(^\circ)$
1	E	$0.015\,\mathrm{A{\cdot}m}$	2.5 2.5 0	90	90
2	E	$0.01\,\mathrm{A{\cdot}m}$	−3 −3 0	90	−45
3	E	$0.01\,\mathrm{A{\cdot}m}$	4 −4 0	45	45
4	M	$2.5 \cdot 10^{-5}\,\mathrm{A{\cdot}m^2}$	1 −1 0	−60	−60
5	M	$2.8 \cdot 10^{-5}\,\mathrm{A{\cdot}m^2}$	−0.9 −0.9 0	0	0
6	M	$2.8 \cdot 10^{-5}\,\mathrm{A{\cdot}m^2}$	2.9 −2.9 0	45	0

4.1. The Electromagnetic Inverse Method Based on the Genetic Algorithms

We know that the classic inverse method uses GA to determine the parameters of radiating sources. In our case, the total number of parameters is 42. When determining all these parameters, the convergence of GA is not realized. Thus, to ensure the convergence of the method, we are obliged to set manually some parameters such as the types of dipoles and their positions. As a result, the convergence is obtained after a simulation time of 51,600 seconds.

Figure 8(a) shows the cartography of the vertical component of the magnetic field obtained at a height of 2 cm, using the real dipoles parameters. However, Figure 8(b) shows the cartography of the vertical component of the magnetic field obtained at the same height, using parameters calculated with the inverse method. We notice that these two cartographies are identical.

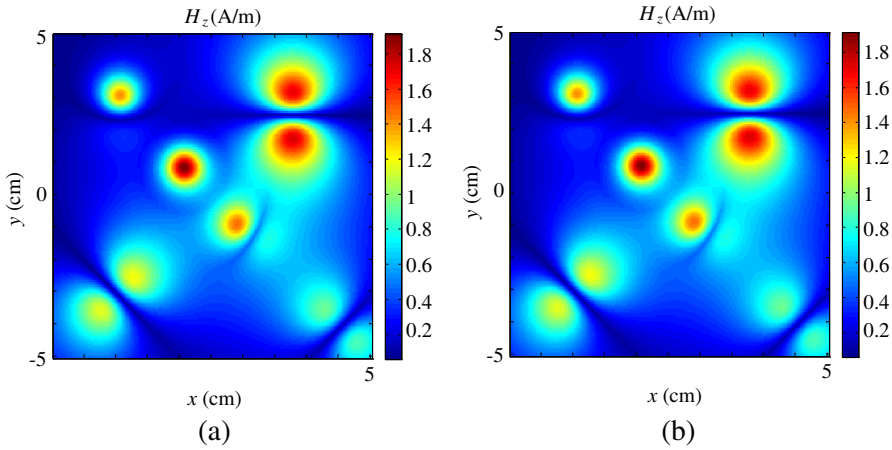

Figure 8. (a) The calculated cartography. (b) The estimated cartography.

4.2. The Proposed Approach

The computation time of the classical electromagnetic inverse method is very important. To overcome this problem, we propose to improve this method by coupling it with the PZMI and the NN, as described in Section 3 of this paper. In fact, we propose to identify only a single dipole. First of all, the identification of the dipole type and position is performed using the PZMI and the NN. Then, the GA method identifies other parameters (the excitation and the orientation). After that, we calculate the field emitted by the obtained dipole over the entire cartography surface. Finally, we will subtract the calculated cartography from the initial one.

Table 5 presents, in details, the processing time of the proposed approach. We notice that our method has successfully identified all the dipole parameters in a simulation time equal to 1,169 seconds which is

Table 5. The processing time.

Step	processing time(s)	Number of iterations
The scan-window	0.000015	28900
PZMI+ANN	0.011713	2890
GA	183.6	6
Total time	1168.98 s	

44 times lower than that obtained in the case of the classical method. In fact, as described above the computing time of the classical method is equal to 51,600 seconds and its convergence is requires manual setting of some parameters such as the types of dipoles and their positions.

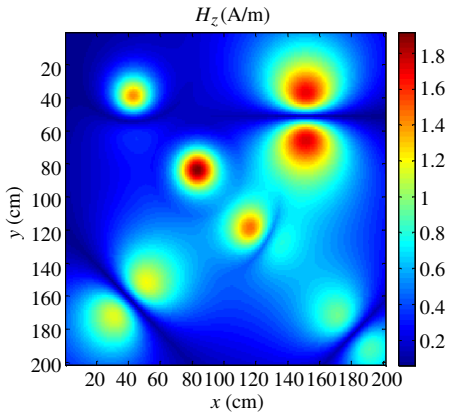

Figure 9. The H_z field estimated by the new proposed approach.

Table 6. The parameters of dipoles.

classic electromagnetic inverse method					
N	T_d	M_d	X_d, Y_d, Z_d (cm)	θ (°)	φ (°)
1	E	0.01499 A·m	2.5 2.5 0	90.2	90.2
2	E	0.01001 A·m	−3 −3 0	91	−44.8
3	E	0.01 A·m	4 −4 0	45.1	45.1
4	M	$2.501 \cdot 10^{-5}$ A·m^2	1 −1 0	59.9	60.1
5	M	$2.7991 \cdot 10^{-5}$ A·m^2	−0.9 −0.9 0	0	0
6	M	$2.8 \cdot 10^{-5}$ A·m^2	2.9 −2.9 0	45.2	0.1
The proposed method					
N	T_d	M_d	X_d, Y_d, Z_d (cm)	θ (°)	φ (°)
1	E	0.015 A·m	2.49 2.50 0	90	90.1
2	E	0.01 A·m	−3.01 −3 0	90	−45
3	E	0.01 A·m	4 −3.99 0	45	45
4	M	$2.499 \cdot 10^{-5}$ A·m^2	1.02 −1 0	60	60
5	M	$2.8 \cdot 10^{-5}$ A·m^2	−0.9 −0.9 0	0.1	0.5
6	M	$2.8 \cdot 10^{-5}$ A·m^2	2.901 −2.899 0	45	0

Figure 9 shows the H_z magnetic field estimated using the parameters determined with our proposed method. We note that the results obtained with our proposed method have negligible error compared to that obtained with the inverse method. Therefore, the inclusion of the scan-window algorithm has shown a great ability with a resolution time considerably lower than that of the classical inverse method.

Table 6 presents the dipoles parameters obtained with the classical method and the proposed one.

4.3. The Robustness of the Proposed Method

The aim of our technique is to find a set of dipoles that give the same emitted field from a studied system at the near field, rather than to find the dipoles with a high precision. Indeed, our method is intended to be applied on industrial systems constituted by complex geometric structures with the aim of being modelized by a network of dipoles. The NF cartographies of these systems have dimensions of around tens of centimeters. Even in the case where two dipoles are separated by few millimeters, our method is able to determine all the radiating sources with a good accuracy. In order to bring out the robustness of our method, we have applied it to a case study where the distance between dipoles 2 and 6 is equal to 10 mm (these two dipoles are shown in Figure 10(a)). Details about the position of the dipoles are given in Table 7.

Table 7. The position of the 6 dipoles.

No	T_d	M_d	X_d, Y_d, Z_d (cm)	θ (°)	φ (°)
1	E	0.015 A·m	2.5 2.5 0	90	90
2	E	0.01 A·m	2.2 −2.2 0	90	−45
3	E	0.01 A·m	4 −4 0	45	45
4	M	$2.5 \cdot 10^{-5}$ A·m^2	1 −1 0	−60	−60
5	M	$2.8 \cdot 10^{-5}$ A·m^2	−0.9 −0.9 0	0	0
6	M	$2.8 \cdot 10^{-5}$ A·m^2	2.9 −2.9 0	45	0

In the case of microelectronics and integrated circuits, which are usually microscopic in size, to make our method able to identify radiating sources, we have to reduce the scan-window size and the measurement step and make another learning phase.

Figure 10(a) shows the cartography of the vertical component of the magnetic field obtained at the height of 2 cm using the real

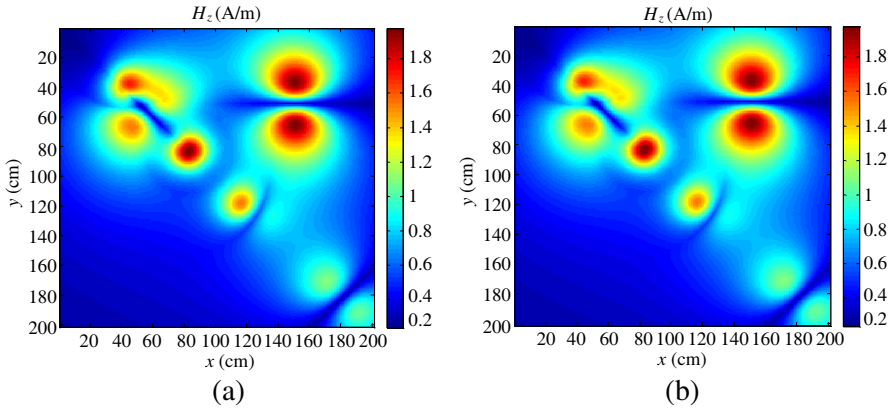

Figure 10. (a) The calculated field. (b) The estimated field.

parameters of the dipoles given in Table 6. In the same figure we plot a line and a circle to represent respectively the electric dipole 2 and the magnetic dipole 6. Figure 10(b) shows the cartography of the vertical component of the magnetic field obtained at the same height, using parameters calculated with the proposed method.

When analyzing the previous cartographies, we confirm that our method has managed to determine the radiating sources from the measured NF with a very good accuracy and in a computation time equal to 918 seconds. Despite the complexity of the previous test, the computation time is less than that spent for the first case because it depends on the initial population used by the GA.

5. CONCLUSION

In spite of the accuracy of the classic electromagnetic inverse method, it presents several disadvantages related to the convergence guarantee of the Genetic Algorithms and the large computation time that they require. To overcome these drawbacks, we propose a new technique based on the PZMI descriptor and the Neural Network.

To validate our approach, we have applied it to a near field cartography emitted by an important number of dipoles.

Among the important contributions of our method are the convergence acceleration while retaining its performance and the presentation of a good robustness. In a further work, we will validate our proposed approach by applying it to measured results of the magnetic field emitted by industrial systems.

REFERENCES

1. Sijher, T. S. and A. A. Kishk, "Antenna modeling by infinitesimal dipoles using genetic algorithms," *Progress In Electromagnetics Research*, Vol. 52, 225–254, 2005.
2. Beghou, L., B. Liu, L. Pichon, and F. Costa, "Synthesis of equivalent 3-D models from near field measurements application to the EMC of power printed circuits boards," *IEEE Transactions of Magnetic*, Vol. 45, No. 3, 1650–1653, Mar. 2009.
3. Vives, Y., C. Arcambal, A. Louis, F. de Daran, P. Eudeline, and B. Mazari, "Modeling magnetic radiations of electronic circuits using near-field scanning method," *IEEE Trans. on EMC*, Vol. 49, No. 2, 391–400, May 2007.
4. Vives, Y., C. Arcambal, A. Louis, R. de Dara, P. Eudeline, and B. Mazari, "Modeling magnetic emissions combining image processing and an optimization algorithm," *IEEE Trans. on EMC*, Vol. 51, No. 4, 909–918, Nov. 2009.
5. Fernandez Lopez, P., C. Arcambal, D. Baudry, S. Verdeyme, and B. Mazari, "Near-field measurements to create a model suitable for commercial simulation tool," *4th Int. Conference on Electromagnetic Near-field Characterization and Imaging (ICONIC)*, 208–213, Taipei, Taiwan, Jul. 2009.
6. Fernandez Lopez, P., C. Arcambal, D. Baudry, S. Verdeyme, and B. Mazari, "Radiation modeling and electromagnetic simulation of an active circuit," *7th Workshop on Electromagnetic Compatibility of Integrated Circuits (EMC Compo 09)*, No. 58, Toulouse, France, Nov. 2009.
7. Ben Hadj Slama, J. and S. Saidi, "Coupling the electromagnetic inverse problem based on genetic algorithms with Moment's method for EMC of circuits," *15th IEEE Mediterranean Electrotechnical Conference, MELECON 2010*, Malta, Italy, Apr. 2010.
8. Liu, B., L. Beghou, L. Pichon, and F. Costa, "Adaptive genetic algorithm based source identification with near-field scanning method," *Progress In Electromagnetics Research B*, Vol. 9, 215–230, 2008.
9. Regue, J. R., M. Ribo, J. M. Garrel, S. Sorroche, and J. Ayuso, "A genetic algorithm based method for predicting far-field radiated emissions from near-field measurements," *IEEE International Symposium Electromagnetic Compatibility*, 147–157, 2000.
10. Fan, H. and F. Schlagenhaufer, "Near field-far field transformation for loops based on genetic algorithm," *CEEM'2006*, 475–481,

Dalian, 2006.

11. Perez, J. R. and J. Basterrechea, "Near to far-field transformation for antenna measurements using a GA based method," *IEEE Antennas and Propagation Society International Symposium*, 734–737, Department of Communications Engineering, ETSIIT, University of Cantabria, 2002.
12. Saidi, S. and J. Ben Hadj Slama, " Effect of genetic algorithm parameters on convergence the electromagnetic inverse method," *International Multi-conference on Systems, Signals & Devices, SSD 2011*, Sousse, Tunisia, Mar. 22–25, 2011.
13. Zhang, H., Z. Dong, and H. Shu, "Objects recognition by a complete set of pseudo-Zernike moment invariants," *ICASSP 2010*, Dallas, Texas, USA, Mar. 14–19, 2010.
14. Saidi, S. and J. Ben Hadj Slama, "The PZMI and artificial neural network to identify the electromagnetic radiation sources," *16th IEEE Mediterranean Electrotechnical Conference, MELECON 2012*, Hammamet, Tunisia, Mar. 2012.
15. Lakshmic Deepika, C., A. Kandaswamy, C. Vimal, and B. Sathish, "Invariant feature extraction from fingerprint biometric using pseudo Zernike moments," *International Journal of Computer Communication and Information System (IJCCIS)*, Vol. 2, No. 1, ISSN: 0976–1349, Jul.–Dec. 2010.
16. Zhu, H., M. Liu, H. Ji, and Y. Li, "Combined invariants to blur and rotation using Zernike moment descriptors," *Pattern Analysis & Applications*, Springer, 2010.
17. Hornik, K., "Approximation capabilities of multilayer feed forward networks," *Neural Networks*, Vol. 4, 251–257, 1991.
18. Wierenga, B. and J. Kluytmans, "Neural nets versus marketing models in time series analysis: A simulation studies," *Proceedings of the 23 Annual Conference, European Marketing Association*, 1139–1153, Maastricht, 1994.